Electrical Power and Energy Systems 176 (2026) 111704

Contents lists available at ScienceDirect

International Journal of Electrical Power and Energy Systems

journal homepage: www.elsevier.com/locate/ijepes

A reservation-based hybrid electric vehicle energy supply system via direct and asynchronous vehicle-to-vehicle charging modes

Yue Cao [a,b], Jixing Cui [a], Shuohan Liu [c,d,*], Xu Zhang [e], Lexi Xu [f], Hongjian Sun [g]

[a] School of Cyber Science and Engineering, Wuhan University, Wuhan, 430072, China
[b] State Key Laboratory of Autonomous Intelligent Unmanned Systems, 100081, Beijing, China
[c] Key Laboratory of Computing Power Network and Information Security, Ministry of Education, Shandong Computer Science Center (National Supercomputer Center in Jinan), Qilu University of Technology (Shandong Academy of Sciences), Jinan, China
[d] Shandong Provincial Key Laboratory of Computing Power Internet and Service Computing, Shandong Fundamental Research Center for Computer Science, Jinan, China
[e] School of Computing Sciences, University of East Anglia (UEA), Norwich, UK
[f] China Unicom Research Institute, Beijing, China
[g] Department of Engineering, Durham University, Durham, DH1 3LE, UK

ARTICLE INFO

Keywords:
Electric energy
Electric vehicle (EV)
Vehicle-to-vehicle (V2V) charging
EV charging optimization
Hybrid V2V charging

ABSTRACT

Electric vehicles, powered by environmentally-friendly electricity, are rapidly emerging as a sustainable alternative to traditional fuel vehicles. However, challenges like range anxiety, stemming from their limited range and prolonged charging times, hinder their widespread adoption. Traditional plug-in charging, limited by rigid charging station deployments, often fails to address the dynamic needs of drivers. To solve this, a novel direct vehicle-to-vehicle charging approach via parking locations has been introduced. In this setup, vehicles act both as energy consumers and providers, forming dynamic peer-to-peer charging pairs. While the direct vehicle-to-vehicle mode is flexible, its effectiveness is curtailed by its inherently low charging power. To remedy this, this paper proposes an asynchronous vehicle-to-vehicle charging scheme via power-storage stations, which are equipped with high-capacity batteries and robust converters. Moreover, this paper proposes a reservation-based hybrid vehicle-to-vehicle charging scheme that integrates both charging modes. Using a real-time reservation system, it can precisely forecast occupancy at parking locations and power-storage stations, ensuring optimal charging by employing the shortest finish time strategy. Simulations validate the efficacy of the proposed scheme, highlighting significant improvements in reducing waiting times and increasing the number of fully charged vehicles compared to existing methods, while buffering energy and shifting service away from demand peaks to support peak shaving and improved asset utilization.

1. Introduction

Electric Vehicles (EVs) have emerged as a key solution to reducing the environmental impact of fossil fuel-powered transportation, aligning closely with the integration of clean energy sources. As a cornerstone of sustainable urban mobility, EVs offer significant potential for lowering greenhouse gas emissions and improving air quality. Nevertheless, their limited driving range remains a critical barrier to widespread adoption. To address this, various energy replenishment strategies have been explored to support reliable and efficient EV operation in urban environments, while remaining compatible with power-system objectives such as peak shaving, distribution-level flexibility, and efficient asset utilization.

The most widely adopted method for energy replenishment in electric vehicles is the plug-in charging mode, with the work in [1] detailing recent station planning advances and the work in [2] reporting operation-side evidence, where vehicles are charged either at home or at charging stations connected to the power grid. Despite the rapid growth in CS deployment, the limited availability of CSs in urban regions remains a major drawback [3], often resulting in prolonged waiting times and reducing the practicality of EVs for daily commuting [4]. Moreover, unlike refueling conventional vehicles, plug-in charging requires significantly more time, which can be inconvenient for users with tight schedules [5], and it may concentrate demand

* Corresponding author at: Key Laboratory of Computing Power Network and Information Security, Ministry of Education, Shandong Computer Science Center (National Supercomputer Center in Jinan), Qilu University of Technology (Shandong Academy of Sciences), Jinan, China.

E-mail addresses: yue.cao@whu.edu.cn (Y. Cao), shuohan.liu@qlu.edu.cn (S. Liu), x.zhang27@uea.ac.uk (X. Zhang), davidlexi@hotmail.com (L. Xu), hongjian.sun@durham.ac.uk (H. Sun).

https://doi.org/10.1016/j.ijepes.2026.111704
Received 29 May 2025; Received in revised form 17 December 2025; Accepted 13 February 2026
Available online 27 February 2026

temporally, leading to queues and suboptimal utilization of charging assets at the distribution level.

Battery swapping offers an alternative solution, wherein depleted batteries are replaced with fully charged ones at dedicated stations [6]. This approach significantly reduces charging time and alleviates the waiting burden [7]. However, it demands standardized battery formats and tight hardware–software integration across vehicle models, leading to high deployment costs and limited scalability in urban contexts, as well as nontrivial coordination with local grid operations.

In comparison, a Vehicle-to-Vehicle (V2V) charging mode, which aligns with smart urban transportation systems, has been proposed in [8] to relieve range anxiety by enabling direct energy transfer between EVs. Under the direct V2V charging mode, Electric Vehicles acting as energy consumers (EV-Cs) and energy providers (EV-Ps) exchange energy at Parking Locations (PLs). In addition, an asynchronous V2V mode [9] allows EV-Cs to receive energy from Power Storage Stations (PSSs), with EV-Ps discharging to PSSs in advance to temporally decouple the exchange; this buffering can shift service away from demand peaks and thus better align with power-system operations.

One major advantage of direct V2V charging is its convenience. With direct V2V charging, drivers can recharge their EVs in a peer-to-peer manner, which makes EVs more practical for everyday use and alleviates the dependence on charging infrastructure. However, since the majority of works under the direct V2V charging service are with low charging power (e.g., generally <20 kW see [10,11] for representative implementations), the charging time through direct V2V charging can last for several hours. Meanwhile, the V2V charging service suffers from uncertainty in EV charging demand, therefore such uncertainty creates huge challenge in pairing EV-Cs and EV-Ps in spatial and temporal dimensions. In our previous work [9], we proposed an asynchronous V2V charging mode that addresses these challenges. It leverages PSSs to temporally decouple energy exchange between EV-Cs and EV-Ps. However, the asynchronous V2V charging inevitably reduces some of the spatial flexibility due to the fixed locations of PSSs.

In this paper, we propose a reservation-based hybrid V2V charging system that integrates direct V2V charging at PLs with asynchronous V2V charging via PSSs. Unlike prior studies that consider either direct or asynchronous/storage-backed charging in isolation, we couple both modes through an explicit reservation–capacity mechanism. We optimize the V2V charging service with a focus on system-level performance measures that are also meaningful to power-system stakeholders (e.g., waiting time, number of fully charged vehicles, energy transferred). The main innovations of this article are as follows:

- **Hybrid V2V Charging Mode & Mode Decision Algorithm:** While previous works have adopted either direct [12,13] or asynchronous [14,15] V2V charging as a supplement to plug-in charging (given that V2V does not burden the grid), our approach integrates both modes. Specifically, direct V2V charging is enabled at PLs, while asynchronous charging is provided via PSSs. To support this, we propose a novel Shortest Finish Time (SFT) algorithm that guides EV-Cs to the optimal mode and site in real time, which helps reduce queueing and completion time and thereby improves effective utilization of charging resources.
- **Reservation-Based System with PSS Recharging:** Prior works have used offline algorithms [16,17] to estimate PL occupancy, but such methods lack real-time accuracy. To address this, we design an online reservation mechanism where EVs actively submit reservation requests, enabling more accurate predictions for both PLs and PSSs. Additionally, instead of relying on grid power, we introduce a dynamic charging and discharging scheme for PSSs based on an Energy Prioritization Strategy (EPS); by buffering energy and scheduling service through reservations, the system can shift load away from peaks and support grid-friendly operation.

In Section 2, we review related work. Section 3 presents the preliminaries. In Section 4, we introduce the framework of our design in detail. Section 5 reports the performance evaluation, and Section 6 presents the conclusion.

2. Related work

The work in [8] introduced an innovative V2V charging approach which allows two EVs to exchange energy directly instead of depending on traditional plug-in charging services. This V2V technique proves to be both cost-effective and convenient. It can also assist in load balancing on the grid during peak hours by sourcing energy from provider vehicles at the time of service rather than the distribution feeder. However, [8] does not consider reservation mechanisms or explicit station capacity/queue modeling, which we address. Furthermore, the work in [18] proposed a dual-input single-output DC-DC converter specifically designed to facilitate the V2V charging service (hardware-centric enablement, scheduling and reservation are out of scope). The work in [19] introduced a series of verification protocols designed for V2V charging services. The core motivation behind this concept lies in furnishing EVs with charging capabilities through the utilization of established standards like dedicated short-range communication, Wi-Fi Direct, or Bluetooth. The authors employed a shared key exchange protocol that does not rely on certificates for authentication. Subsequently, they designed protocols utilizing smartphones in conjunction with Wi-Fi Direct standards . Here, the focus is on authentication/verification rather than queue-aware scheduling or capacity planning.

Within the framework of V2V charging services, two primary applications are under study: direct and asynchronous V2V charging modes. In the typical direct V2V charging approach, EVs are categorized into pairs, consisting of EV-Ps and EV-Cs. To facilitate the exchange of energy between them, specialized energy transfer devices such as DC-DC converters [20] are employed (direct V2V commonly operates at relatively low charging power, e.g., <20 kW in practice).

In contrast, under the asynchronous V2V charging mode, energy accumulators located at PSSs serve as intermediaries. They accumulate energy from the providers and subsequently transmit it to EV-Cs in need of charging. As a result, in the asynchronous V2V charging scenario, the charging and discharging processes can occur without requiring the simultaneous presence of both EVs. This temporal decoupling increases feasible power delivery but reduces spatial flexibility due to fixed station locations.

2.1. Direct vehicle-to-vehicle charging mode

Under the direct V2V charging service, when an EV-C requests for charging, it requires an adequate energy provider to match for a maximized charging utility and minimized charging cost. The optimization framework for direct V2V charging is divided into V2V-Pair (formed by EV-Cs with EV-Ps) Matching and PL-Selecting.

- **V2V-Pair Matching:** Bulut et al. [16] introduced a V2V charging system designed to facilitate energy transfer between EVs. This system allows EV drivers experiencing range anxiety to purchase excess energy from other EVs. The communication among EVs is established through a location-based social networking system. To optimize the pairing of EVs, they employed a maximum weighted bipartite matching algorithm. Here, reservations and station capacity/queue effects are not modeled, differing from our hybrid, queue-aware design. In a separate study by Kabir et al. [21], a company operates a fleet of charging trucks, each outfitted with a sizeable battery and a rapid charger, enabled for V2V charging service. Their primary objective is to maximize the number of fully charged EVs served. Additionally, the study accounts for the requirement that all trucks must return to the depot after serving EVs. To address this, the authors formulated an Integer Linear Programming (ILP) model to determine the optimal trajectory for each truck. This truck-routing focus contrasts with our station-capacity-aware scheduling of direct and asynchronous modes. The work in [17] focuses on allocating EV-Cs to suitable suppliers (CSs or energy providers) to minimize the overall charging cost. This matching problem is represented as a mixed integer optimization problem, known to be NP-hard, and is solved using the stable marriage algorithm. Here, asynchronous buffering at storage stations and flow-time-oriented scheduling are not considered.

- **PL-Selecting:** Generally, when EV-Cs and EV-Ps are engaged in V2V-Pair matching, they often encounter the challenge of PL-Selecting. Once the Global Controller (GC) completes a feasibility analysis of PL-Selecting for V2V-Pairs, several key factors come into play, including trajectory driving time, energy consumption, charging duration, and Charging Quality of Experience (QoE). In practical scenarios, EVs require an optimized PL-Selecting process due to the limited availability of parking resources. Additionally, PLs may not always have sufficient equipment or chargers for V2V charging services. Surprisingly, only a handful of prior studies have taken into account the combined problem of PL-Selecting alongside V2V-Pair matching [22] , and queue/capacity constraints are typically simplified. A communication framework, grounded in a vehicular ad-hoc network, is devised to facilitate real-time data transmission between CSs and EVs [23]. Utilizing the calculated travel energy cost and charging QoE model, EVs can reserve the optimal PL, minimizing charging costs. Furthermore, an efficient V2V charging navigation strategy for EVs, based on vehicle communication, is proposed in [22]. Firstly, an effective semi-centralized charging navigation structure based on mobile edge computing is established. It ensures the reliable billing information dissemination and feasible charging coordination, with a low cost of communication and computation. Upon this, authors designed an effective local-to-global charging navigation mechanism, to dynamically select the driving route and PL for V2V charging operation. However, asynchronous storage-backed operation is not integrated.

2.2. Asynchronous vehicle-to-vehicle charging mode

In contrast to the direct V2V charging approach, the asynchronous V2V charging method allows EV-Cs and EV-Ps to initiate V2V charging independently, eliminating the need for simultaneous charging. In this scenario, energy providers transmit energy to PSS stations equipped with stationary energy storage (e.g., battery systems) [24], which store the energy. The PSS can then transfer this stored energy to EV-Cs whenever required.

Furthermore, in the study described in [25], SAE J1772 combo connectors are utilized between EVs to facilitate energy transfer, coupled with 60 kW DC-to-AC power converters. In the context of asynchronous V2V charging services, when an EV driver requests charging, the GC allocates an appropriate PSS to maximize the charging efficiency while minimizing the charging duration. This optimization challenge can be broken down into two key components: PSS-Selection and PSS-Scheduling.

- **PSS-Selecting:** Kim et al. [26] addressed the challenges of range anxiety and limited charging infrastructure by employing matching theory to efficiently pair energy suppliers with energy consumers. In their paper, authors introduced a method grounded in matching theory that facilitates collaboration between Vehicle-to-Grid (V2G) and V2V charging modes. This approach aims to alleviate range anxiety and increase the number of charged EVs. It explicit reservation and queue–capacity coupling are not considered. Similarly, the work in [27] proposed a hybrid V2V and Grid-to-Vehicle (G2V) mode. In this configuration, EVs that submit charging requests are centrally allocated by the GC to charge either at CSs using the G2V mode or at PLs through V2V interactions. The most advantageous charging choice between CSs and PLs is determined through the analysis of two distinct service queues, aimed at minimizing the charging costs for the EVs. Here, asynchronous buffering at storage stations and SFT scheduling are not included. To compute the charging expenses, the Analytical Hierarchy Process is employed, which takes into account factors such as charging waiting time, charging price, and charging energy, assigning appropriate weights. Moreover, a charging reservation method is put into practice to evaluate charging availability and guarantee a favorable QoE for drivers.
- **PSS-Scheduling:** During the PSS-Scheduling phase, scheduling algorithms assume a pivotal role in efficiently overseeing the charging and discharging processes of EVs. Yuan et al. [28] delved into the complexities of EV charging scheduling, examining it through the lens of V2V auctions and local generation. Their work is situated within the context of demand response strategies. To incentivize EVs to participate in energy supply, the authors introduced an online auction mechanism that leverages a primal–dual approximation algorithm. This innovative approach breaks down the long-term social cost minimization problem into a series of single-round auctions. Additionally, to alleviate the expenses associated with frequent switching of local generators, the authors devised an online algorithm inspired by the concept of delayed switching. Importantly, this online algorithm ensures provable polynomial running time, authenticity, and individual rationality for each auction. However, the study does not integrate hybrid direct/asynchronous operation or SFT reservation scheduling. On a related note, Koufakis et al. [29] proposed an optimal EV charging scheduling scheme that takes into account the synergy between G2V and V2V charging modes. This research formulates the optimization using ILP and tackles problem solving in an offline fashion. Furthermore, it introduces three distinct optimal configurations for EV charging planning, designed to facilitate energy transfer between EVs Here, reservation-based, queue-aware scheduling with storage buffering is not the focus.

To situate our contribution, Table 1 contrasts representative schemes along five axes algorithmic paradigm (online vs. offline), operation mode (direct, asynchronous, or direct + asynchronous), reservation mechanism, capacity modeling, and optimization objective. The comparison shows that ours is the only online approach that integrates hybrid operation (direct + asynchronous) with explicit reservation–capacity coupling; most prior work either addresses a single operation mode or lacks integrated capacity management. (Here, “hybrid” refers to the operation mode, not to an algorithmic mix of online and offline optimization.)

3. Preliminaries

3.1. Assumptions

In this article, we propose a hybrid V2V charging system designed for urban environments. The system includes a GC that centrally manages charging by communicating with EVs, PLs, and PSSs. Multiple PLs and PSSs are geographically distributed and equipped with DC-DC converters to support concurrent energy transfer. Each PL and PSS provides a finite service capacity (parallel converters).

The EVs are divided into three categories: EV-Cs, EV-Ps, and EV Trucks (EV-Ts). They start at a different speed while traveling with a constant speed. The freshness of EVs occupation status information, critical for V2V charging, is determined by the communication architecture. To achieve this, the GC, EVs, PLs, and PSSs are equipped with a wireless communication module that allows low-latency communication through the cellular network. Additionally, encrypted communication is applied between the EVs and the GC to ensure that the message is not intercepted by unauthorized entities and to protect drivers’ privacy.

Table 1
Comparison of recent EV energy-supply schemes and this work

Reference	Mode	Reservation	Capacity	Objectives	Scope relative to this work
[8]	Direct	No	No queue/capacity modeling	Cost; feasibility	*Scope:* peer-to-peer V2V feasibility; *Our focus:* reservation & capacity aware hybrid scheduling
[16]	Direct	No	No queue/capacity modeling	Maximum-weight matching	*Scope:* social-graph pairing; *Our focus:* hybrid scheduling with reservations and capacity constraints
[22]	Direct	Yes (PL)	Limited capacity	Navigation; QoE	*Scope:* reservation-based PL navigation; *Our focus:* integrates storage-backed asynchronous mode and capacity-aware scheduling
[18]	Direct	No	Not modeled	Converter design	*Scope:* hardware enablement & prototype; *Our focus:* system level scheduling
[26]	V2G+V2V	Implicit	Limited capacity	Matching	*Scope:* V2G+V2V matching; *Our focus:* explicit reservation coupling and hybrid mode
[27]	V2V+G2V	Yes (CS/PL)	Two queues	Cost; QoE	*Scope:* central allocation between CS and PL; *Our focus:* storage buffering and SFT reservations
[29]	V2G+V2V	No	Some capacity modeling	Offline ILP optimality	*Scope:* offline planning; *Our focus:* online reservation scheduling at city scale
This work	Hybrid (direct+async)	Yes	Yes; capacity modeled	Waiting time; QoE; peak shaving	*Scope:* hybrid direct & asynchronous with reservation- and capacity-aware SFT scheduling

3.2. Network entity

- **Global Controller (GC):** It orchestrates the coordination of EV-related data, and computes real-time information to manage the charging and discharging allocation of EVs.
- **EV-Cs:** Upon detecting a State Of Charge (SOC) that is sub-threshold, the EV-C initiates a charging request to the GC and awaits the delineation of charging allocation.
- **EV-Ps:** They generally random travel in network only if they have not been paired (with EV-Cs and PSSs). EV-Ps will discharge to EV-Cs or PSSs when receiving arrangement information from the GC.
- **EV-Ts:** In addition to EV-Ps, we introduce EV-Ts with higher battery capacity to supplement electric quantity in the central area. Due to their limited mobility (low travel speed), EV-Ts are only assigned to provide energy to PSSs in the central area, as described in Section 5.1.
- **PLs:** PLs can provide the direct V2V charging services using their parking lots. EVs can be charged/discharged using direct V2V converters equipped at PLs.
- **PSSs:** PSSs can provide the asynchronous V2V charging services. They are equipped with stationary battery storage to retain energy offloaded from EV-Ps/EV-Ts and subsequently provide asynchronous charging services to EV-Cs.

3.3. Proposed reservation-based hybrid V2V charging system

This paper presents a novel reservation-based hybrid V2V charging mode that combines both direct and asynchronous modes to improve system efficiency. The direct V2V charging mode utilizes DC-DC converters installed at PLs to match EV-Cs and EV-Ps for charging. The asynchronous V2V charging mode utilizes PSSs with DC-DC converters to transfer power between EV-Cs and EV-Ps/EV-Ts [18]. Here, one direction of energy transferring is from PSSs to EV-Cs, while the other direction of energy transferring is from EV-Ps/EV-Ts to PSSs.

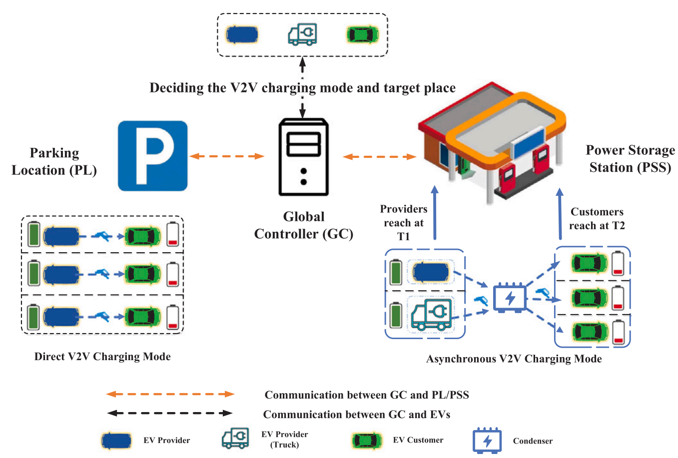

Fig. 1. Toy example of the reservation-based hybrid V2V system: the GC compares a PL (direct V2V) and a PSS (asynchronous V2V) by estimating the expected completion time under each option, and selects the mode/site for two illustrative requests (at $T1$ and $T2$).

3.3.1. Toy example: Scenario of the reservation-based hybrid V2V charging decision Walk-through

Fig. 1 provides an illustrative toy example of how the proposed reservation-based hybrid V2V system operates. We consider two EV-Cs that trigger charging requests at different times (denoted as $T1$ and $T2$ in the figure), and assume they may target the same nearby PL or PSS. Upon receiving a request, the GC collects real-time information from both EVs and fixed infrastructure (PLs and PSSs), including travel status, current occupancy, and the expected availability of V2V converters.

The GC then compares two options. In the direct V2V mode (PL), service can start only after the EV-C and the selected EV-P arrive at the same parking location, so the decision is affected by possible

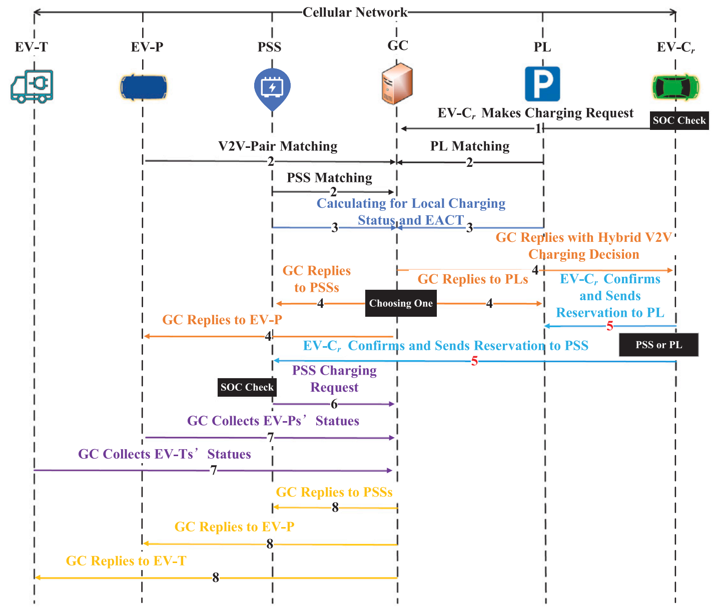

Fig. 2. Time sequence for the hybrid V2V charging service.

synchronization delay between the two EVs. In the asynchronous mode (PSS), the customer can start charging once it arrives at the station, but it may experience waiting due to limited converter capacity and existing reservations. Based on these anticipated delays and service durations, the GC selects the charging mode and the target location that yields the earliest expected completion, and informs the EV-C to place a reservation at the chosen PL/PSS.

3.3.2. Time sequence of the reservation-based hybrid V2V charging system

Fig. 2 illustrates the time sequence of the proposed reservation-based hybrid V2V charging mode. First, when the SOC of EV-C$_r$ falls below a predefined threshold, it sends a charging request to the GC. Next, the GC collects real-time information on available EV-Ps, PSSs, and PLs. It then computes the local charging status, including queue length and reservation data, and estimates the Earliest Available Charging Time (EACT) for both PSSs and PLs (see Section 4.3). Subsequently, the GC determines the appropriate charging mode and notifies the relevant entities (EV-P and PL, or PSS) for service matching. Finally, EV-C$_r$ confirms the GC's recommendation. If direct V2V charging is selected, it sends a reservation to the target PL; otherwise, it reserves the assigned PSS for asynchronous charging.

The above sequence is for recharge process of EV-C$_r$, but PSSs also require recharging when their SOC are below the threshold. As steps 6–8 in Fig. 2, when a PSS needs charging, it sends a request to the GC. Based on the online calculation results about status of EV-Ps and EV-Ts (detailed in Section 4.7), the GC informs the selected EVs for recharging PSS.

3.4. Problem formulation

Problem setting: Charging requests arrive over time. At the current decision epoch T^{cur}, the system observes the real-time status of all sites (occupancy/workload and capacity) and the travel information of the arriving EV-C. The goal is to assign each arriving EV-C to either a PL (direct V2V) or a PSS (asynchronous V2V) to minimize its expected completion time under finite-capacity constraints.

To alleviate V2V charging congestion and improve charging efficiency, we formulate a hybrid V2V charging management problem. The following notations are defined:

- γ: Total service time for an EV-C to complete charging at PLs/PSSs, including both waiting and charging durations [s].
- τ: Average waiting time per EV-C from arrival to charging initiation [s].
- $N_{PL/PSS}$: Total number of PLs and PSSs in the network.
- ω: Number of EV-Cs arriving at PLs/PSSs during the simulation.
- Ω: Aggregate charging service time for all EV-Cs [s].
- $\mathcal{R}$: set of arriving EV-Cs;
- $\mathcal{M} = N_{\mathrm{PL/PSS}}$: candidate sites (PLs and PSSs).
- k_m: number of parallel V2V converters at site m (finite capacity).
- $DIS_{r,m}$ [m]: distance from EV-C r to site m; v_r [m/s]: EV-C speed.

At PLs, the waiting time of an EV-C may be caused by delayed EV-P arrival or limited converter availability, whereas at PSSs, it is solely due to converter constraints. Queues are handled logically (predicted) and respect finite capacity k_m; the delay enters the model via a site-dependent queueing term $W_{r,m}$ [s].

System objective: We assign each arriving EV-C$_r$ to a site $m_r \in \mathcal{M}$ (PL or PSS) to minimize the sum of predicted completion times

$$\min_{\{m_r \in \mathcal{M}\}} \sum_{r \in R} F_{r,m_r} \quad [\mathrm{s}], \tag{1}$$

where $F_{r,m}$ is the predicted finish time if r chooses site m.

Feasibility and constraints: We use binary assignment variables $x_{r,m} \in \{0,1\}$ with $\sum_{m\in\mathcal{M}} x_{r,m} = 1$ for each r, and $m_r = \arg\max_m x_{r,m}$. The processing time is

$$p_{r,m} = \frac{E_r^{\max} - E_r^{cur}}{\alpha_m} \times 3600 \quad [\mathrm{s}] \quad (\mathrm{kWh/kW} \to \mathrm{h} \to \mathrm{s}), \tag{2}$$

where α_m is the site charging power. The travel-based arrival is $a_{r,m} = T^{cur} + \frac{DIS_{r,m}}{v_r}$ [s]. Let $p(r)$ denotes the EV-P paired with EV-C$_r$. Then $a_{p(r),m}$ represents the predicted arrival time of the provider at site, calculated analogously to $a_{r,m}$. For PLs, charging can only start after *both* vehicles arrive, so we set the effective start time $\tilde{a}_{r,m} \geq \max\{a_{r,m}, a_{p(r),m}\}$; for PSSs, $\tilde{a}_{r,m} \geq a_{r,m}$. Then, $W_{r,m} \geq 0$ denotes the predicted queueing delay at site m. To estimate $W_{r,m}$, we define L_m as the total remaining service workload at site m, including all ongoing and queued EVs as of time T^{cur}. The delay is then approximated by

$$W_{r,m} = \frac{L_m}{k_m} \quad [\mathrm{s}], \tag{3}$$

where k_m is the number of parallel converters at site m. This queueing-inspired term captures capacity-induced waiting under finite parallel converters and is incorporated into the finish-time prediction to support online mode/site decisions under congestion. The approximation assumes that the remaining workload is evenly distributed across the k_m service units. Accordingly, the predicted finish time is

$$F_{r,m} = \left(\tilde{a}_{r,m} - T^{cur}\right) + W_{r,m} + p_{r,m} \quad \text{[s]}. \tag{4}$$

Finite capacity is enforced implicitly because $W_{r,m}$ is derived from the ongoing workloads under k_m parallel servers. Note that $\omega_i = \sum_r \mathbf{1}[m_r = i]$ is the *realized* inflow induced by $\{m_r\}$ and is not a decision variable.

Online site choice (SFT-based): For an arriving EV-C r, we evaluate $F_{r,m}$ over a pre-filtered candidate set and select

$$m_r^\star = \arg\min_{m\in\mathcal{M}} F_{r,m}. \tag{5}$$

Connection to the waiting-time form: If site powers are homogeneous ($\alpha_m \equiv \alpha$) and travel-time differences are negligible (e.g., after proximity pre-filtering), minimizing $F_{r,m}$ is equivalent to minimizing the predicted waiting time. In this special case, the online choice reduces to the original waiting-time form below.

$$\arg\min_{m\in N_{PL/PSS}} \tau_m := \{m \mid \tau_m < \tau_i, \forall i \in N_{PL/PSS}\}. \tag{6}$$

In essence, the goal is to assign each EV-C to a PL or PSS such that its expected completion time (travel + queueing + service) is minimized with all quantities expressed in SI units (distance in m, speed in m/s, time in s). The SFT rule implements this objective in an online fashion without invoking reservation-specific constructs in the formulation.

3.5. Queueing-theoretic and matching-theoretic foundation

The hybrid system's performance derives from two complementary mechanisms: **Asynchronous Mode (GI/G/k Queueing Model):** Each PSS with k_m converters operates as a $GI/G/k_m$ queue. The expected waiting time $E[W_q]$ scales with utilization $\rho = \lambda/(\mu k_m)$, service time $E[S]$, and variability measures. SFT improves performance by:

1. Reducing effective $E[S]$ via high-power PSS assignment
2. Load balancing across stations (implicit JSQ policy)

Direct Mode (Synchronization-Constrained Matching): PL delays are dominated by *pair-arrival synchronization latency*, not classical queueing. This matches stochastic rendezvous problems where delay depends on spatial agent distribution. SFT dynamically avoids synchronization bottlenecks by:

$$\text{Switch to PSS if} \quad \underbrace{\max(T_C^{\text{arr}}, T_P^{\text{arr}})}_{\text{Sync delay}} > \underbrace{W_{r,\text{PSS}} + p_{r,\text{PSS}}}_{\text{PSS queueing}} \tag{7}$$

4. System framework and algorithm

4.1. Framework of system

Fig. 3 illustrates the framework of the reservation-based hybrid V2V charging system. EV-Cs would initiate recharging requests when its SOC falls below the threshold. Then, EV-Cs maintain information by Algorithm 1 and Algorithm 2. The information about the local occupation of PLs and PSSs can be obtained, to calculate the earliest available charging time of PL (PL-EACT) and the earliest available charging time of PSS (PSS-EACT), illustrated by Algorithm 3 in Section 4.3. Then, the EACT information is fed into the hybrid V2V charging decision.

Based on the information from Algorithms 1–3, two charging modes will be compared to choose the optimal one (Algorithm 4 in Section 4.4). The hybrid V2V charging decision is made based on the information gathered from the PL and PSS service recommendations. The GC calculates the optimal V2V charging mode using the SFT based algorithm. Then, the GC informs the EV-C of the target PL/PSS and the chosen V2V charging mode. Afterwards, the EV-C makes charging reservation by sending request to the target PL/PSS after receiving the information from the GC.

If there are EVs at a PL, the PL schedules arriving and reservation V2V-Pairs according to a scheduling algorithm (Algorithm 5 in Section 4.6). PSSs can be recharged under the asynchronous V2V charging when its SOC is below the threshold. Afterwards, the PSS will send a recharging request for EV-Ps/EV-Ts to request supplement. The algorithm of PSS recharging is described in detail by Algorithm 6 in Section 4.7. PSS schedules arriving and reservation EVs according to the scheduling algorithm (by Algorithm 7 in Section 4.7).

4.2. Charging information collection

Upon receiving the request, the GC will calculate the information of the two V2V charging modes using Algorithms 1 and 2 for EV-C_r (the certain EV needs V2V charging when its SOC is below the threshold).

Algorithm 1 V2V-Pair Matching and PL Matching

1: **for** $(i = 1; i \le N_P; i++)$ **do**
2:   **if** (EV-P_i is not matched) **then**
3:     Calculate DIS_{P_i,C_r}
4:   **end if**
5: **end for**
6: Target EV-P ← arg min(DIS_{P_i,C_r})
7: **for** $(j = 1; j \le N_{PL}; j++)$ **do**
8:   Calculate DIS_{PL_j,C_r}
9:   LIST_{PL}.ADD(DIS_{PL_j,C_r})
10: **end for**
11: Sort LIST_{PL} in ascending order
12: **return** LIST_{PL}

Algorithm 2 PSS Matching

1: **for** $(i = 1; i \le N_{PSS}; i++)$ **do**
2:   Calculate DIS_{PSS_i,C_r}
3:   LIST_{PSS}.ADD(DIS_{PSS_i,C_r})
4: **end for**
5: Sort LIST_{PSS} in ascending order
6: **return** LIST_{PSS}

- In the case of direct V2V charging, EV-C_r is paired with the nearest EV-P_i (where i in the number of PLs N_{PL}) to conduct energy exchange at a PL. Algorithm 1 performs this pairing by identifying the EV-P with the minimum distance to EV-C_r (lines 1–6), where DIS_{P_i,C_r} denotes the distance between EV-P_i and EV-C_r. Subsequently, it computes the distances between EV-C_r and all PLs (lines 7–10), stores them in LIST_{PL}, and returns the sorted list in ascending order of distance.
- In the case of asynchronous V2V charging, EV-C_r is matched to a PSS_i (where i in the number of PSSs N_{PSS}). In Algorithm 2, lines 1–4 compute the distance DIS_{PSS_i,C_r} between each PSS and EV-C_r, storing the results in LIST_{PSS}. At line 5, LIST_{PSS} is sorted in ascending order of distance. The sorted list is then returned for subsequent decision-making.

4.3. Estimation of EACT with reservation

Algorithm 3 estimates the EACT with the reservation at PL/PSS. If there is none EV being charged, Algorithm 3 returns the current time T^{cur} at line 2. Between lines 4–6, Algorithm 3 calculates the charging finish time of EVs under recharged and adds results to the LIST_{EACT}. Here, N_C is the number of EVs being charged, LIST_{EACT} is the LIST of EACT at PLs/PSSs. Here, $E_{C_i}^{\max}$ is the maximum battery capacity (kWh) and $E_{C_i}^{cur}$ is the current energy (kWh) of EV-C_i (in the queue of N_C). α is the charging power (kW). Thus $T^{cha} = 3600\,(E^{\max} - E^{cur})/\alpha$ returns seconds (s).

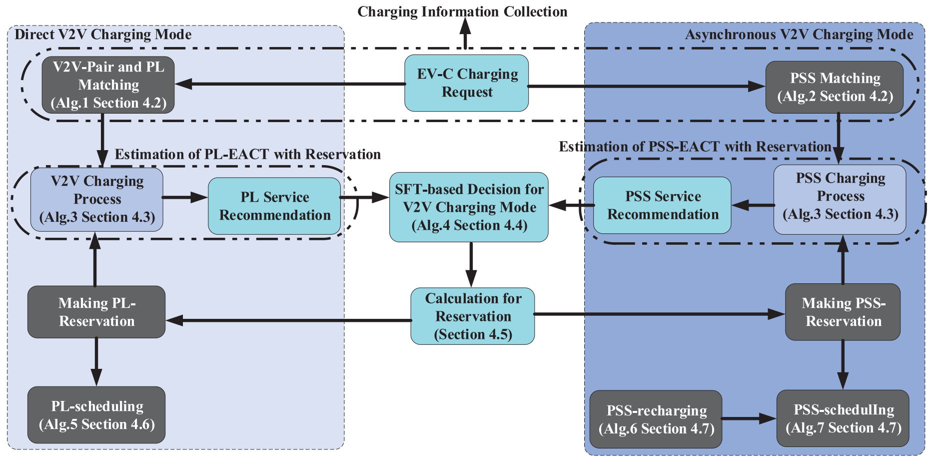

Fig. 3. Framework of the hybrid V2V charging service.

Algorithm 3 Estimation of EACT with Reservation

1: **if** (If no EV is being charged) **then**
2: **return** T^{cur}
3: **end if**
4: **for** $(i = 1; i \le N_C; i++)$ **do**
5: LIST$_{EACT}$.ADD($T^{cur} + \frac{E^{max}_{C_i} - E^{cur}_{C_i}}{\alpha}$)
6: **end for**
7: **if** (LIST$_{EACT}$.SIZE() $< N^{Slot}$) **then**
8: Add T^{cur} to LIST$_{EACT}$ with (N^{Slot} - LIST$_{EACT}$.SIZE()) times
9: **end if**
10: Sort LIST$_{EACT}$ in ascending order
11: Sort the queue of N_W according to FIFS order
12: **for** $(j = 1; j \le N_W; ++j)$ **do**
13: LIST$_{EACT}$[0] += $\frac{E^{max}_{C_j} - E^{cur}_{C_j}}{\alpha}$
14: Sort LIST$_{EACT}$ in ascending order
15: **end for**
16: **for** $(k = 1; k \le N_R; k++)$ **do**
17: **if** $(T^{arr}_{C_k} < T^{arr}_{C_r})$ **then**
18: $T^{cha}_{C_k} = \frac{E^{max}_{C_k} - E^{cur}_{C_k}}{\alpha}$
19: $T^{fin}_{C_k} = T^{cha}_{C_k}$ + LIST$_{EACT}$[0]
20: Replace LIST$_{EACT}$[0] with $T^{fin}_{C_k}$
21: Sort LIST$_{EACT}$ in ascending order
22: **end if**
23: **end for**
24: **return** LIST$_{EACT}$[0] as the EACT

If the charging slots are not fully occupied given by the condition (LIST$_{EACT}$.SIZE() $< N^{Slot}$), T^{cur} will be added to the LIST$_{EACT}$ with (N^{Slot} - LIST$_{EACT}$.SIZE()) times at line 8.

Between lines 12–15, Algorithm 3 calculates the charging finish time of waiting EVs (N_W is the number of EVs waiting for charging) and adds results to the LIST$_{EACT}$. The LIST$_{EACT}$[0] is added with charging time of EV-C$_j$ (in the queue of N_W) at line 13. Here, LIST$_{EACT}$[0] is the earliest available charging time at PL/PSS, $\frac{E^{max}_{C_j} - E^{cur}_{C_j}}{\alpha}$ is charging duration time for EV-C$_j$.

Between lines 16–24, the charging finish time of those EVs in the queue of N_R are calculated and added to LIST$_{EACT}$. If the arrival time of EV-C$_r$ is later than the reservation EV-C$_k$ (in the queue of N_R) given by the condition (arrival time of EV-C$_k$ is earlier than EV-C$_r$, $T^{arr}_{C_k} < T^{arr}_{C_r}$), EV-C$_r$ can be charged until the time EV-C$_k$ finishing charging. Specifically, the charging time denoted by the charging duration time ($T^{cha}_{C_k}$) of EV-C$_k$ is calculated at line 18. Here, the ($E^{max}_{C_k} - E^{cur}_{C_k}$) is energy for EV-C$_k$ needed to be charged. Then, the charging finish time of EV-C$_k$ ($T^{fin}_{C_k}$) is calculated as ($T^{cha}_{C_k}$ + LIST$_{EACT}$[0]). As the LIST$_{EACT}$ contains the EACT of EVs, the LIST$_{EACT}$[0] is EACT of EV completed service in the LIST$_{EACT}$. Afterwards, the LIST$_{EACT}$[0] is replaced by $T^{fin}_{C_k}$ to imply that the first available converter is occupied by EV-C$_k$ until $T^{fin}_{C_k}$. Then, the LIST$_{EACT}$ is sorted in ascending order at line 21. Finally, Algorithm 3 returns LIST$_{EACT}$[0] as the EACT, which means that EV-C$_r$ needs to wait for the available slot and converter until time EACT at PL/PSS.

4.4. SFT-based decision for V2V charging mode

At time T^{cur}, the SFT decision uses the observable state of the arriving EV-C$_r$ (position and speed v_r, current/maximum energy E^{cur}_r, $E^{\max}_r$), the pre-filtered candidate sets LIST$_{PL}$ and LIST$_{PSS}$, each site's charging power α_m, and the site's earliest-available charging time T^{EACT}_m derived from current workloads and k_m parallel converters. For direct V2V at PLs, the provider's predicted arrival $T^{arr}_{P_r}$ is also needed so the pair arrival is $\max\{T^{arr}_{C_r}, T^{arr}_{P_r}\}$. From these inputs we compute the travel-based start time $\tilde{a}_{r,m}$, the processing time $p_{r,m} = \frac{E^{\max}_r - E^{cur}_r}{\alpha_m}$ (converted to seconds), and thus the predicted finish time $F_{r,m} = (\tilde{a}_{r,m} - T^{cur}) + W_{r,m} + p_{r,m}$. The procedure outputs exactly what is required for subsequent reservation and scheduling: the selected mode (Direct vs. Asynchronous), the chosen target site $m^\star_r = \arg\min_m F_{r,m}$, and the associated shortest-finish-time value $F_{r,m^\star_r}$. All time quantities are expressed in seconds (distance in meters, speed in m/s; kWh/kW is converted to seconds).

All quantities use SI units: distances DIS (m) and speeds (m/s) yield arrivals/travel times T^{arr} (s), the charging time $T^{cha}_{C_r} = \frac{E^{max}_{C_r} - E^{cur}_{C_r}}{\alpha}$ is computed as (kWh)/(kW)→h and then reported in seconds, so all SFT terms are in seconds. The earliest-available time T^{EACT} from Algorithm 3 already accounts for the finite number of parallel converters at each site (finite capacity). Per request the algorithm evaluates at most 2δ candidates (PLs and PSSs), i.e., $O(\delta)$ work plus fetching T^{EACT}; with $\delta = 5$ and fixed per-site capacity in our experiments, the per-request runtime is small and stable.

Based on results from Algorithm 1–3, EV-C$_r$ can execute one V2V charging mode by executing SFT-based decision in Algorithm 4. Between lines 1–13, the SFT of δ number PLs nearby is calculated. In order to optimize the computational complexity, δ number of objects nearby are selected for calculation.

Specifically, at line 3, the time that EV-C$_r$ travels to arbitrary PL$_i$ (belongs to the δ number of nearby PLs) is calculated by $\frac{DIS_{C_r,PL_i}}{Speed_{C_r}}$ (DIS is in meters and $Speed$ in m/s, yielding seconds). The arrival time of EV-C$_r$ at PL$_i$ is calculated by ($\frac{DIS_{C_r,PL_i}}{Speed_{C_r}} + T^{cur}$).

Then, the matched EV-P for EV-C$_r$ is needed for considered. The arrival time of the EV-P at PL$_i$ is calculated at line 4. Due to the direct V2V charging can be started until both the V2V-Pair has arrived, the arrival time of the V2V-Pair (T^{arr}_{pair}) is the later time between EV-C$_r$ and

Algorithm 4 SFT-based Decision

1: **for** $(i = 1; i \le \delta; i++)$ **do**
2: The PL_i is fetched from the $LIST_{PL}$ ← Algorithm 1
3: $T^{arr}_{C_r} = \frac{DIS_{C_r,PL_i}}{Speed_{C_r}} + T^{cur}$
4: $T^{arr}_{P_r} = \frac{DIS_{P,PL_i}}{Speed_{P_r}} + T^{cur}$
5: $T^{arr}_{pair} = \max(T^{arr}_{C_r}, T^{arr}_{P_r})$
6: $T^{EACT}_{PL_i}$ ← Algorithm 3
7: $T^{cha}_{C_r} = \frac{E^{max}_{C_r} - E^{cur}_{C_r}}{\alpha}$
8: **if** $(T^{arr}_{pair} < T^{EACT}_{PL_i})$ **then**
9: $SFT_{PL_i} = (T^{EACT}_{PL_i} - T^{cur}) + T^{cha}_{C_r}$
10: **else**
11: $SFT_{PL_i} = (T^{arr}_{pair} - T^{cur}) + T^{cha}_{C_r}$
12: **end if**
13: The shortest finish time at the PL $(SFT^{min}_{PL}) = \arg\min(SFT_{PL_i}, SFT^{min}_{PL})$
14: **end for**
15: **for** $(j = 1; j \le \delta; j++)$ **do**
16: The PSS_j is fetched from the $LIST_{PSS}$ ← Algorithm 2
17: $T^{tra}_{PSS_j} = \frac{DIS_{C_r,PSS_j}}{Speed_{C_r}}$
18: $T^{EACT}_{PSS_j}$ ← Algorithm 3
19: $T^{cha}_{C_r} = \frac{E^{max}_{C_r} - E^{cur}_{C_r}}{\alpha}$
20: **if** $(T^{arr}_{C_r} < T^{EACT}_{PSS_j})$ **then**
21: $SFT_{PSS_j} = (T^{EACT}_{PSS_j} - T^{cur}) + T^{cha}_{C_r}$
22: **else**
23: $SFT_{PSS_j} = T^{tra}_{PSS_j} + T^{cha}_{C_r}$
24: **end if**
The shortest finish time at the PL $(SFT^{min}_{PSS}) = \arg\min(SFT_{PSS_j}, SFT^{min}_{PSS})$
25: **end for**
26: **if** $(SFT^{min}_{PSS} < SFT^{min}_{PL})$ **then**
27: EV-C_r proceeds recharging under the Asynchronous V2V Charging Mode
28: **else**
29: EV-C_r proceeds recharging under the Direct V2V Charging Mode
30: **end if**

EV-P at line 5. At line 6, the EACT of PL_i is calculated by Algorithm 3. Then, EV-C_r's charging time at PL_i is calculated by $\frac{E^{max}_{C_r} - E^{cur}_{C_r}}{\alpha}$ at line 7.

- Especially, if the arrival time of the V2V-Pair is earlier than the EACT time of PL_i, EV-C_r can start V2V charging until $T^{EACT}_{PL_i}$. Thus, the SFT of PL_i is calculated by $(T^{EACT}_{PL_i} - T^{cur} + T^{cha}_{C_r})$. Specifically, $(T^{EACT}_{PL_i} - T^{cur})$ is the waiting time for an available slot and $T^{cha}_{C_r}$ is the charging time for EV-C_r.
- Otherwise, the SFT of PL_i is calculated by $(T^{arr}_{pair} - T^{cur} + T^{cha}_{C_r})$ at line 11. Here, $(T^{arr}_{pair} - T^{cur})$ means that V2V-Pair can start direct V2V charging as arriving at the target PL.

Afterwards, the minimum SFT of PL is given by the condition ($\arg\min(SFT_{PL_i}, SFT^{min}_{PL})$) at line 13. Thus, with results between lines 1–14, the minimum SFT of δ number PLs nearby can be calculated. With the same algorithmic logic, the minimum SFT of δ number PSSs nearby is calculated between lines 15–25. At line 26, if the minimum SFT of PSSs is smaller than that of PLs, i.e., $SFT^{\min}_{PSS} < SFT^{\min}_{PL}$, EV-$C_r$ proceeds with asynchronous V2V charging, as it is expected to experience a shorter service waiting time. Otherwise, EV-C_r opts for direct V2V charging. Intuitively, dispatching EV-Cs by the minimum predicted finish time (including travel, queueing, and service) is a non-preemptive shortest completion time rule, which is known to reduce aggregate flow-time in many single/parallel-server settings.

Our objective is to minimize $\sum_{r\in\mathcal{R}} F_{r,m_r}$, selecting $m_r = \arg\min_m F_{r,m}$ at each decision epoch is a standard list-scheduling step. By a two-job interchange at a fixed site, serving the job with smaller F first does not increase the sum of completion times, so the SFT choice is locally dominant. We do not claim global optimality for unrelated parallel machines with release dates, but this provides a principled link between the heuristic and the objective while respecting finite capacity via $W_{r,m}$. Because the travel component enters $F_{r,m}$ explicitly, SFT only chooses a farther site when the projected reduction in queueing + /or service time exceeds the extra travel; hence detour cost remains bounded by the δ-candidate prefilter and justified by net completion-time gains.

4.5. Calculation for reservation

If EV-C_r proceeds the direct V2V charging in Algorithm 4, it will send a reservation to the target PL. The time that EV-C_r arrives at the target PL is calculated by $(T^{cur} + \frac{DIS_{C_r,PL}}{Speed_{C_r}})$, where $Speed_{C_r}$ is the traveling speed for EV-C_r. Similarly, the time that EV-P arrives at the PL is calculated by $(T^{cur} + \frac{DIS_{P,PL}}{Speed_P})$, where $Speed_P$ is the traveling speed for the EV-P (note that we assume the EV-P and EV-T are with different speed in Section 3.1). Then, the arrival time of EV-C_r and EV-P are compared to determine the reservation time:

- **Case 1:** If EV-C_r arrives at the target PL before the EV-P, it must wait until the EV-P arrives to initiate V2V charging. In this case, the reservation time is set to the arrival time of the EV-P.
- **Case 2:** If EV-C_r arrives at the target PL after the EV-P, it can begin charging immediately upon arrival. The reservation time is equal to EV-C_r's arrival time.

Afterwards, the expected remaining energy when EV-C_r arrives at the target PL is calculated by $(E^{cur}_{C_r} - \beta \times DIS_{C_r,PL})$, where $E^{cur}_{C_r}$ is the current energy of EV-C_r. Here, the β is the energy consumption rate of EV-C while driving. Then, EV-C_r makes a reservation to the target PL with information on reservation time, max battery capacity and expected remaining energy.

If EV-C_r proceeds the asynchronous V2V charging in Algorithm 4, it will send a reservation to the target PSS. The arrival time of EV-C_r is calculated by $(T^{cur} + \frac{DIS_{C_r,PSS}}{Speed_{C_r}})$. Under the asynchronous V2V charging mode, since EV-C_r is charged by PSSs without EV-Ps, the reservation time of EV-C_r is equal to the arrival time of EV-C_r. The expected remaining energy when EV-C_r arrives at the target PSS is calculated by $(E^{cur}_{C_r} - \beta \times DIS_{C_r,PSS})$. Then, EV-$C_r$ makes a reservation to the target PSS with information on reservation time, max battery capacity and expected remaining energy.

4.6. PL-scheduling

Algorithm 5 PLs schedule EVs under Direct V2V Charging

1: Sort the $LIST_{wait}$ with FIFS Algorithm
2: **for** $(i = 1; i \le N_W; i++)$ **do**
3: **if** ($LIST_{cha}$.SIZE() $< N^{Slot}_{PL}$) **then**
4: $LIST_{cha}$.ADD(V2V-$Pair_i$)
5: $LIST_{wait}$.REMOVE(V2V-$Pair_i$)
6: **end if**
7: **end for**
8: PL executes service as $LIST_{cha}$ under the Direct V2V Charging Mode

When there are V2V-Pairs at a PL needed to execute the direct V2V charging service, the PL will schedule V2V-Pairs charging according to Algorithm 5. Firstly, Algorithm 5 schedules those V2V-Pairs waiting for available charging converters in waiting list of EVs ($LIST_{wait}$) according to First In First Serve (FIFS) scheme at line 1. Here, $LIST_{wait}$ is the waiting list of EVs at the PL. Secondly, between lines 2–7, the PL adds V2V-Pairs to the charging LIST ($LIST_{cha}$) when there is available V2V charging slots given by the condition ($LIST_{cha}$.SIZE() < the number of charging slot of the PL (N^{Slot}_{PL})). Then, V2V-Pairs in $LIST_{wait}$ will be removed at line 5. Afterwards, the PL executes service as $LIST_{cha}$ under the direct V2V charging mode.

Algorithm 6 PSS-recharging

1: **if** (The SOC of PSS is below threshold) **then**
2: **for** ($i = 1; i \le N_P; i++$) **do**
3: **if** (EV-P_i is not matched) **then**
4: $LIST_{rec}$.ADD(DIS_{PSS,P_i})
5: **end if**
6: **end for**
7: **if** (The PSS is located in the central area) **then**
8: **for** ($j = 1; j < N_T; j++$) **do**
9: **if** (EV-T_j is not matched) **then**
10: $LIST_{rec}$.ADD(DIS_{PSS,T_j})
11: **end if**
12: **end for**
13: **end if**
14: Sort $LIST_{rec}$ in ascending order
15: $M = N^{Slot}_{PSS_r}$
16: The first M EVs in the $LIST_{rec}$ make reservation to the PSS
17: The PSS will be recharged by the first M EVs in the $LIST_{rec}$
18: **end if**

4.7. PSS-scheduling

Under the asynchronous V2V charging mode, a PSS needs to recharge if its energy is at a low level (the details are explained in Section 3.3 and steps 6–8 in Fig. 2). In Algorithm 6, if the SOC of the PSS is below the threshold, the PSS will find EV-Ps/EV-Ts to recharged. Between lines 2–6 in Algorithm 6, the PSS maintains the recharging list of EV-Ps/EV-Ts for PSSs ($LIST_{rec}$). Here, $LIST_{rec}$ is the recharging list of EV-Ps/EV-Ts for the PSS.

At line 3, if EV-P_i (where i belongs to N_P) is not matched, the PSS adds the distance from EV-P_i to $LIST_{rec}$. Furthermore, if the PSS is located in the central area (defined in Section 5.1), it can be recharged by EV-Ts as the high demand for electricity. Moreover, due to the low mobility but high energy capacity of EV-Ts, EV-Ts are beneficial for reducing battery anxiety in the central area. Between lines 8–12, The GC adds the distance between PSS and EV-T_j (where j belongs to the number of EV-Ts N_T) to $LIST_{rec}$. Then, the $LIST_{rec}$ is sorted in ascending order at line 14. At line 16, the first M EVs in the $LIST_{rec}$ will make reservation to the PSS. Finally, at line 17, the PSS will be recharged by the first M EVs in the $LIST_{rec}$, where M is the number of charging slots at the PSS (N^{Slot}_{PSS}).

Algorithm 7 PSSs schedule EVs under Asynchronous V2V Charging

1: **if** (The SOC of PSS is below threshold) **then**
2: PSS runs Algorithm 6
3: Sort the $LIST_{wait}$ with EPS scheme
4: **else**
5: Sort the $LIST_{wait}$ with FIFS Algorithm
6: **end if**
7: **for** ($i = 1; i \le N_W; i++$) **do**
8: **if** ($LIST_{cha}$.SIZE() $< N^{Slot}_{PSS}$) **then**
9: $LIST_{cha}$.ADD(EV_i)
10: $LIST_{wait}$.REMOVE(EV_i)
11: **end if**
12: **end for**
13: PSS executes EV-Cs for charging service as $LIST_{cha}$ under the Asynchronous V2V Charging Mode

In Algorithm 7, in case that the SOC of the PSS is higher than the threshold and there are EVs at the PSS needed to execute the asynchronous V2V charging service, the $LIST_{wait}$ will be sorted with FIFS Algorithm. Otherwise, if the SOC of the PSS is below the threshold, the PSS sorts the $LIST_{wait}$ with EPS scheme. In EPS algorithm, EV-Ps/EV-Ts will be prioritized to charge PSS by occupying charging converters, rather than supplying EV-Cs charging.

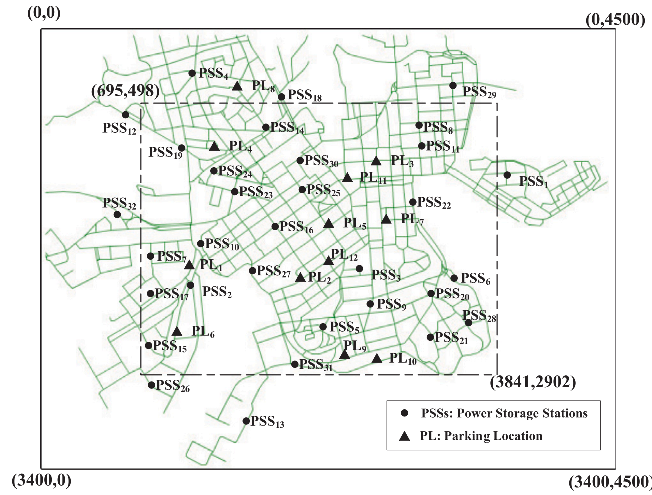

Fig. 4. Simulation map (Helsinki): study area and road network with PLs and PSSs, where trajectories are generated within the boxed region.

Afterwards, the PSS schedules the asynchronous V2V charging service for EVs. Between lines 7–12, if there are free charging slots given by the condition ($LIST_{cha}$.SIZE() $< N^{Slot}_{PSS}$), the PSS adds EV_i (in the queue of N_W) to the $LIST_{cha}$ and removes it from the $LIST_{wait}$. Here, the $LIST_{cha}$ contains EVs is under the asynchronous V2V charging. Then, the PSS executes EVs as $LIST_{cha}$ under the asynchronous V2V charging mode.

5. Performance evaluation

5.1. Simulation configuration

Fig. 4 presents the simulation environment for V2V charging within a 4500 m × 3400 m area of Helsinki, Finland, constructed using the Opportunistic Network Environment (ONE). The central region, outlined by the dotted box, is bounded by coordinates $695 < X < 3841$ and $498 < Y < 2902$, covering approximately half of the city. A total of 32 PSSs and 12 PLs are deployed to support hybrid V2V charging services. EV-Cs and EV-Ps move at variable speeds between 30 and 50 km/h, while EV-Ts are restricted to the central area and travel at speeds of 20 to 30 km/h.

Three EV-C types are configured as follows:

- Coda Automotive: 33.8 kWh battery, 193 km range, 30% SOC.
- Wheego Whip: 30 kWh battery, 161 km range, 40% SOC.
- Hyundai BlueOn: 16.4 kWh battery, 140 km range, 50% SOC.

For example, the Coda Automotive EV-Cs have an initial energy of 33.8 kWh and an endurance mileage of 193 km, with an energy SOC threshold set at 30%. In contrast, the EV-Ps have an initial energy of 60 kWh, while the EV-Ts have 120 kWh, allowing them to provide unlimited energy to feed EV-Cs at PSSs during the simulation. Each PL/PSS is equipped with 8 V2V DC-DC converters to enable V2V energy transfer in parallel, but the charging power differs between PL and PSS.

Currently, charging piles are capable of delivering a charging power that surpasses 100 kW. While the charging capacity of V2V mode might not reach the 100 kW threshold, the unparalleled convenience they offer, along with other associated advantages, sets them apart from regular charging piles. Specifically, the charging power achievable through V2V technology exceeds 40 kW [30], allowing for efficient charging of EVs within a remarkably short span of 1–2 h. This rapid charging capability significantly reduces the downtime of EVs and supports seamless, on-the-go charging experiences for drivers. Here, the charging power at the PL is 20 kW (within the 6–22 kW range reported for direct V2V prototypes [31]), while the charging power at PSS is 40 kW (mid-range for stationary DC converters [32]). Unless otherwise noted, all reported points are the mean over three independent random seeds. To avoid clutter, the main plots show means. The simulation lasts for 12 h.

The following are V2V charge schemes and performance indicators:

- **Direct V2V (Distance)** [33]**:** Prioritizes spatial efficiency by selecting V2V pairs and PLs based on minimum geographical distance.
- **Direct V2V (Duration)** [34]**:** Focuses on temporal efficiency by minimizing V2V charging service duration during pair and PL selection.
- **Asynchronous V2V (Distance):** Operates in asynchronous mode with PSS scheduling based on the low-SOC-first charging principle.
- **Hybrid V2V (MWT)** [9]**:** Combines direct and asynchronous modes; allocates charging by minimizing waiting time and applies LSFC for PSS scheduling.
- **Hybrid V2V (Reservation-based SFT):** The proposed scheme introduces reservations and a SFT strategy to dynamically switch between modes, ensuring energy stability via EPS in asynchronous charging.

The considered performance metrics are as follows:

- **Number of EVs Fully Charged (NOFC):** This metric denotes the total count of services that all EVs achieve fully charging throughout the simulation period, serving as an indicator from the perspective of the system.
- **Average Waiting Time (AWT):** This metric denotes the average queueing delay that an EV spends waiting to be fully charged upon arriving at the chosen PSS, serving as an indicator from the perspective of EVs.
- **Energy Transferred (ET):** This metric denotes the total energy delivered to EV-Cs during the simulation, i.e., the sum over all completed charging sessions.
- **Detour Cost (DC):** This metric denotes the additional EV travel relative to the nearest feasible site at the decision time, measured as extra distance or travel time aggregated across requests.
- **Converter Utilization (U):** This metric denotes the fraction of time converters are occupied; we compute it per site and report the converter-count–weighted average across all sites.

5.2. Investigation on parameters setting

Parameter sensitivity (EV-T count): Before conducting the comparison experiment, we conducted simulations to optimize the number of EV-Ts and the selection of compared stations parameters. Specifically, we varied the number of EV-Cs from 0 to 90 in increments of 30, and after 12 h of simulation, we analyzed the results of the influence of the EV-Ts' number, as shown in Fig. 5(a) and 5(b).

The results in Fig. 5(a) show that the use of EV-Ts leads to improved performance, as they can bring a significant amount of energy. However, as the number of EV-Ts increased, we observed that the improvement reaches saturation. On the other hand, Fig. 5(b) shows that the performance of AWT is worse when there are more than 60 EV-Ts, the main reason is that much more EV-Ts cause congestion at PSSs and leads to increased waiting time of EV-Cs. Based on these findings, we set the number of EV-Ts to 30 for the following simulation experiments with concern to minimize the cost of additional energy supplier operated in network.

Parameter sensitivity (number of candidate stations δ): We conducted simulations by varying the number of nearby stations (δ) from 1 to 10. The results are shown in Fig. 6(a) and 6(b). Our findings indicate that the performance of the scheme is better when the number of stations is set to 5, as it outperforms other settings in terms of AWT and NOFC. Thus, we set the number of nearby stations (δ) to 5 for the later simulation experiments.

5.3. Influence of EVs density

In reality, the number of EVs has a significant impact on the load of the charging system, which in turn affects the quality of charging services. Therefore, we conducted a simulation experiment to simulate the increase in EV density.

5.3.1. Influence of EV-Cs density on AWT and NOFC

We set the count of EV-Ps at 180 and EV-Ts at 30. To investigate the adaptability of four V2V schemes to a rising number of EV-Cs, we varied the EV-Cs count from 90 to 360 in increments of 90.

Fig. 7(a) shows that under both Direct V2V (Distance) and Direct V2V (Duration) schemes, NOFC declines as the number of EV-Cs increases, due to limited EV-P availability and lower charging power. In contrast, the Asynchronous V2V (Distance) scheme achieves better NOFC performance by leveraging high-power converters at PSSs and greater flexibility. However, while it accommodates larger EV-C populations more effectively, its performance remains inferior to that of the Hybrid V2V schemes.

Among the Hybrid V2V schemes, the Reservation-based SFT variant clearly outperforms the MWT-based approach. This advantage arises from the SFT algorithm's ability to reduce charging service duration, thereby increasing the number of EV-Cs served. As a result, the Reservation-based SFT scheme consistently achieves higher NOFC, particularly as the EV-C population grows.

Fig. 7(b) delineates the performance of all V2V charging schemes in terms of AWT. The Direct V2V (Distance) and Direct V2V (Duration) schemes exhibit the highest AWT, a consequence of the limited availability of EV-Ps and subpar charging power. Conversely, the asynchronous V2V charging mode registers a reduced AWT, attributed to the expedited charging facilitated by PSSs. Regarding the hybrid V2V charging modes, the Hybrid V2V (Reservation-based SFT) surpasses the Hybrid V2V (MWT). As elucidated in Algorithm 4, EV-Cs have the option to charge either directly from EV-Ps or asynchronously from PSSs. The decision is predicated on the computed values of SFT^{min}_{PL} and SFT^{min}_{PSS}, determining the optimal V2V charging mode based on SFT. Consequently, in terms of AWT, the Hybrid V2V (Reservation-based SFT) demonstrates superior performance, especially with an increasing count of EV-Cs.

As EV-C arrivals increase, baselines show the usual sharp rise in AWT. Reservation-based SFT keeps AWT lower by routing to the earliest-finishing site (leveraging higher-power PSSs), balancing load across PL/PSS, and using reservation timing to cut AWT growth (see Fig. 7(b)) and turning capacity into more completions, hence higher NOFC (see Fig. 7(a)).

Secondary system-level metrics: In addition to NOFC and AWT, we tracked three system-level metrics: ET, DC and U. As expected, ET increases with NOFC (fixed powers/request sizes); DC remains modest because the travel term is penalized inside $F_{r,m}$ and site choice is restricted to the δ nearest candidates; and U rises with throughput while SFT's balancing prevents localized saturation. These secondary metrics thus move consistently with the NOFC/AWT trends, so we keep NOFC and AWT as primary outcomes and summarize the others in text to avoid clutter.

5.3.2. Influence of EV-Ps density on AWT and NOFC

We fix the number of EV-Cs as 360 to simulate the high demand scenario. To explore the response of four V2V schemes to an augmented number of EV-Ps, we adjust the EV-Ps density, ranging from 90 to 360.

As shown in Fig. 8(a), both the Direct V2V (Distance) and Direct V2V (Duration) schemes exhibit lower NOFC performance due to insufficient EV-P supply under high EV-C demand. In contrast, the remaining three schemes — particularly the Hybrid V2V (Reservation-based SFT) — demonstrate greater adaptability as EV-P availability increases. Notably, the Reservation-based Hybrid V2V maintains strong performance even with limited EV-Ps, attributed to its ability to dynamically switch

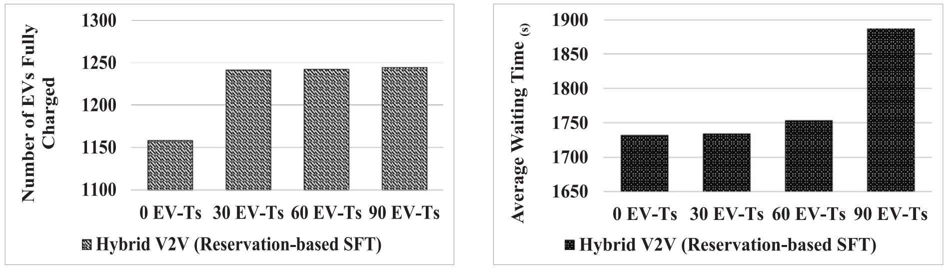

(a) Influence of EV-Ts on NOFC

(b) Influence of EV-Ts on AWT

Fig. 5. Effect of EV-T count on performance: (a) fully charged EVs (NOFC), (b) average waiting time (AWT, s).

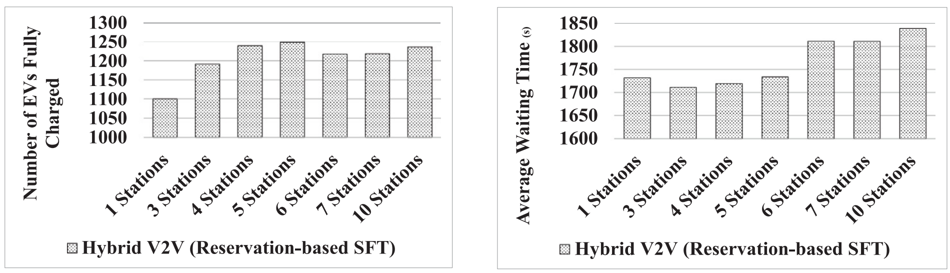

(a) Influence of Stations on NOFC

(b) Influence of Number of Comparison Stations on AWT

Fig. 6. Effect of candidate station number δ: (a) NOFC, (b) AWT (s).

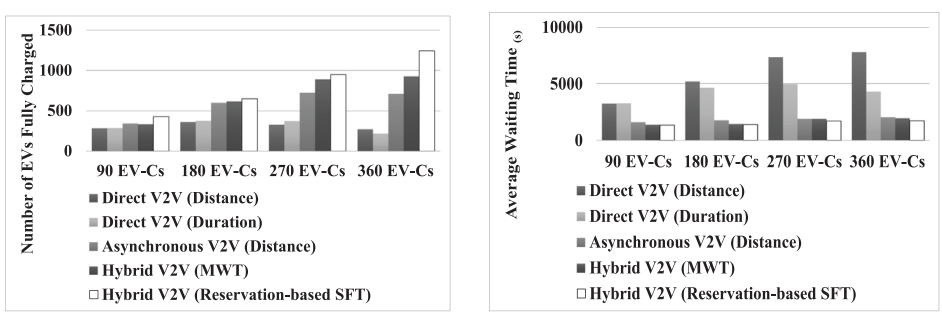

(a) Influence of EV-Cs on NOFC

(b) Influence of EV-Cs on AWT

Fig. 7. Effect of EV-C density on (a) NOFC and (b) AWT (s)

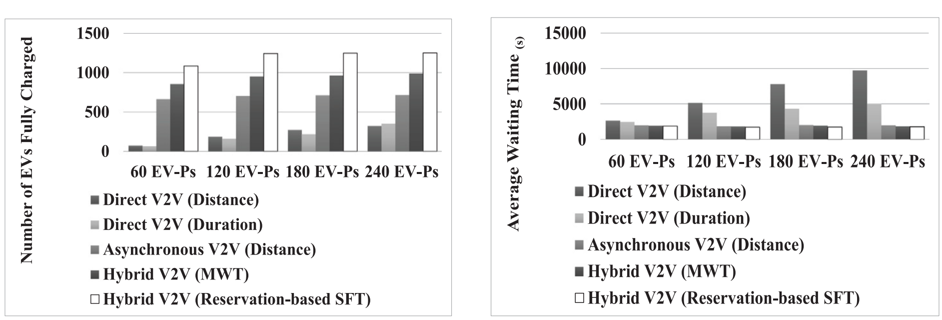

(a) Influence of EV-Ps on NOFC

(b) Influence of EV-Ps on AWT

Fig. 8. Impact of EV-Ps density on (a) NOFC and (b) AWT.

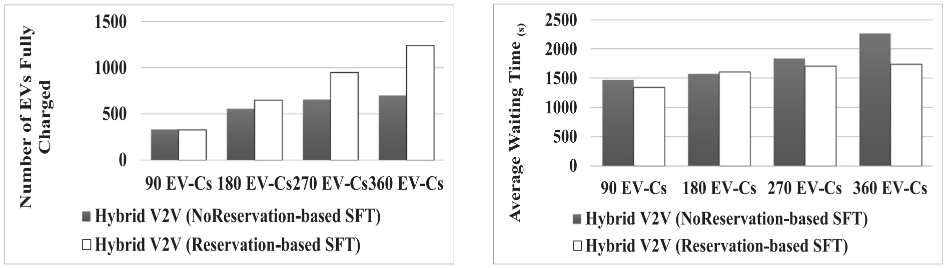

(a) Effect of Reservation on NOFC

(b) Influence of Reservation on AWT

Fig. 9. Comparison of reservation strategy impacts on: (a) NOFC and (b) AWT.

EV-Cs to the optimal charging mode based on reservation-informed scheduling, while efficiently utilizing EV-Ps across both direct and asynchronous modes.

Similarly, Fig. 8(b) shows that the direct V2V schemes suffer from high waiting times under supply constraints. In contrast, the Hybrid V2V (Reservation-based SFT) consistently achieves the shortest average waiting time, owing to its flexible coordination mechanism that balances real-time demand with predictive reservation strategies.

Furthermore, when EV-Ps are scarce, direct V2V at PLs incurs a pair-arrival synchronization delay. SFT detects this and switches EV-Cs to asynchronous PSS service, eliminating the synchronization gate and exploiting higher power, which explains the larger gains in AWT reduction and NOFC in the low-EV-P regime (see Fig. 8(a) & 8(b)). As EV-P availability grows, SFT continues to balance work between PLs and PSSs, maintaining the advantage.

5.4. *Influence of reservation*

To assess the impact of reservation, the number of EV-Ps and EV-Ts is fixed at 180 and 30, respectively, while the number of EV-Cs varies from 90 to 360. This isolates the contribution of the reservation–capacity coupling to system-level performance.

As illustrated in Fig. 9(a), increasing the number of EV-Cs does not lead to severe congestion under either Hybrid V2V scheme. However, the Reservation-based SFT leverages reservation information to anticipate charging hotspots. Consequently, as shown in Fig. 9(b), it consistently outperforms the NoReservation-based SFT in both NOFC and AWT, achieving more fully charged EVs and reduced waiting times. These results substantiate the originality claim that reservations, when coupled with capacity-aware earliest-available-time estimation and SFT assignment, are a key driver of the observed flow-time improvements.

Our reservation-based SFT relies on predicted finish times that combine travel, queueing delay under finite capacity k_m, and service time determined by site power α_m. Hence the dispatch rule is map-agnostic and depends on local EACT/queue dynamics rather than a specific road topology. While we evaluate on a heterogeneous urban map (downtown and peripheral patterns) and average over three seeds with CIs, full multi-map replication is left as future work.

6. Conclusion

Electric vehicles, as a form of electrically powered road transport, are rapidly expanding in adoption. However, many drivers still face range anxiety and queueing at charging infrastructure. Meanwhile, delivering user-centric energy supply while supporting power-system objectives such as peak shaving and asset utilization remains challenging. This study presented a reservation-based hybrid vehicle-to-vehicle energy-supply scheme that integrates direct charging at parking locations with asynchronous charging via power-storage stations. A shortest-finish-time decision rule, informed by reservations and converter capacity, assigns each electric vehicle as energy consumer to the mode and site that minimize expected completion time. In city-scale simulations on the Helsinki road network, the method consistently reduced average waiting time and increased the number of fully charged electric vehicles compared with alternatives, with gains most pronounced under high demand. By buffering energy at storage stations and shifting service away from peaks, the design aligns with power-system goals and improves effective utilization of charging assets. Future work will extend validation across multiple urban maps and random seeds, include parameter-sensitivity studies, and provide analytical bounds that clarify the connection between the decision rule and flow-time minimization.

CRediT authorship contribution statement

Yue Cao: Writing – review & editing, Formal analysis, Conceptualization. **Jixing Cui:** Writing – original draft, Validation, Software, Data curation. **Shuohan Liu:** Writing – review & editing, Writing – original draft, Project administration, Methodology, Conceptualization. **Xu Zhang:** Methodology, Formal analysis. **Lexi Xu:** Supervision, Project administration, Methodology. **Hongjian Sun:** Supervision.

Declaration of competing interest

The authors declare that they have no known competing financial interests or personal relationships that could have appeared to influence the work reported in this paper.

Acknowledgments

This work was supported in part by the State Key Laboratory of Autonomous Intelligent Unmanned Systems. The opening project number is ZZKF2025-1-16 and Hubei Province International Science and Technology Collaboration Program (2025EHA043), the National Natural Science Foundation of China (62501339), the Natural Science Foundation of Shandong Province, China (ZR2025QC713).

Data availability

Data will be made available on request.

References

[1] Kazemtarghi A, Mallik A, Chen Y. Dynamic pricing strategy for electric vehicle charging stations to distribute the congestion and maximize the revenue. Int J Electr Power Energy Syst 2024;158:109946. http://dx.doi.org/10.1016/j.ijepes.2024.109946, URL https://www.sciencedirect.com/science/article/pii/S0142061524001674.

[2] Jiang C, Zhou L, Zheng J, Shao Z. Electric vehicle charging navigation strategy in coupled smart grid and transportation network: A hierarchical reinforcement learning approach. Int J Electr Power Energy Syst 2024;157:109823. http://dx.doi.org/10.1016/j.ijepes.2024.109823, URL https://www.sciencedirect.com/science/article/pii/S0142061524000449.

[3] Richard R, Cao H, Wachowicz M. EVStationSIM: An end-to-end platform to identify and interpret similar clustering patterns of EV charging stations across multiple time slices. Appl Energy 2022;322:119491.
[4] Liu S, Xia X, Cao Y, Ni Q, Zhang X, Xu L. Reservation-based EV charging recommendation concerning charging urgency policy. Sustain Cities Soc 2021;74:103150.
[5] Li H, Li G, Lie TT, Li X, Wang K, et al. Constrained large-scale real-time EV scheduling based on recurrent deep reinforcement learning. Int J Electr Power Energy Syst 2023;144:108603. http://dx.doi.org/10.1016/j.ijepes.2022.108603, URL https://www.sciencedirect.com/science/article/pii/S0142061522005993.
[6] Ahmad F, Saad Alam M, Saad Alsaidan I, Shariff SM. Battery swapping station for electric vehicles: opportunities and challenges. IET Smart Grid 2020;3(3):280–6.
[7] Zhang X, Peng L, Cao Y, Liu S, Zhou H, Huang K. Towards holistic charging management for urban electric taxi via a hybrid deployment of battery charging and swap stations. Renew Energy 2020;155:703–16. http://dx.doi.org/10.1016/j.renene.2020.03.093.
[8] You P, Yang Z. Efficient optimal scheduling of charging station with multiple electric vehicles via V2V. In: 2014 IEEE international conference on smart grid communications. smartGridComm, 2014, p. 716–21. http://dx.doi.org/10.1109/SmartGridComm.2014.7007732.
[9] Cui J, Liu S, Cao Y, Zhang X, Zhou H, Ren X. A hybrid electric vehicle energy supply system via direct and asynchronous V2V charging modes. In: 2022 IEEE international conference on systems, man, and cybernetics. SMC, 2022, p. 2056–61. http://dx.doi.org/10.1109/SMC53654.2022.9945337.
[10] Ucer E, Buckreus R, Kisacikoglu MC, Bulut E, Guven M, Sozer Y, et al. A flexible V2V charger as a new layer of vehicle-grid integration framework. In: 2019 IEEE transportation electrification conference and expo. ITEC, 2019, p. 1–7. http://dx.doi.org/10.1109/ITEC.2019.8790483.
[11] Sousa TJC, Monteiro V, Fernandes JCA, Couto C, Meléndez AAN, Afonso JL. New perspectives for vehicle-to-vehicle (V2V) power transfer. In: IECON 2018 - 44th annual conference of the IEEE industrial electronics society. 2018, p. 5183–8. http://dx.doi.org/10.1109/IECON.2018.8591209.
[12] Abualola H, Otrok H, Mizouni R, Singh S. A V2V charging allocation protocol for electric vehicles in VANET. Veh Commun 2022;33:100427.
[13] Shurrab M, Singh S, Otrok H, Mizouni R, Khadkikar V, Zeineldin H. An efficient vehicle-to-vehicle (V2V) energy sharing framework. IEEE Internet Things J 2021;9(7):5315–28.
[14] Masrur MA, Skowronska AG, Hancock J, Kolhoff SW, McGrew DZ, Vandiver JC, et al. Military-based vehicle-to-grid and vehicle-to-vehicle microgrid—System architecture and implementation. IEEE Trans Transp Electrification 2017;4(1):157–71.
[15] Shah V, Payami S. Integrated converter with G2V, V2G, and DC/V2V charging capabilities for switched reluctance motor drive-train based EV application. IEEE Trans Ind Appl 2023;1–14. http://dx.doi.org/10.1109/TIA.2023.3242636.
[16] Bulut E, Kisacikoglu MC. Mitigating range anxiety via vehicle-to-vehicle social charging system. In: 2017 IEEE 85th vehicular technology conference. VTC spring, 2017, p. 1–5. http://dx.doi.org/10.1109/VTCSpring.2017.8108288.
[17] Zhang R, Cheng X, Yang L. Flexible energy management protocol for cooperative EV-to-EV charging. IEEE Trans Intell Transp Syst 2019;20(1):172–84. http://dx.doi.org/10.1109/TITS.2018.2807184.
[18] Kumar GG, Sundaramoorthy K. Dual-input nonisolated DC–DC converter with vehicle-to-grid feature. IEEE J Emerg Sel Top Power Electron 2022;10(3):3324–36. http://dx.doi.org/10.1109/JESTPE.2020.3042967.
[19] Roberts B, Akkaya K, Bulut E, Kisacikoglu M. An authentication framework for electric vehicle-to-electric vehicle charging applications. In: 2017 IEEE 14th international conference on mobile ad hoc and sensor systems. MASS, 2017, p. 565–9. http://dx.doi.org/10.1109/MASS.2017.93.
[20] B S U, Khadkikar V, Zeineldin HH, Singh S, Otrok H, Mizouni R. Direct electric vehicle to vehicle (V2V) power transfer using on-board drivetrain and motor windings. IEEE Trans Ind Electron 2022;69(11):10765–75. http://dx.doi.org/10.1109/TIE.2021.3121707.
[21] Kabir ME, Sorkhoh I, Moussa B, Assi C. Routing and scheduling of mobile EV chargers for vehicle to vehicle (V2V) energy transfer. In: 2020 IEEE power and energy society general meeting. PESGM, 2020, p. 1–5. http://dx.doi.org/10.1109/PESGM41954.2020.9281674.
[22] Li G, Sun Q, Boukhatem L, Wu J, Yang J. Intelligent vehicle-to-vehicle charging navigation for mobile electric vehicles via VANET-based communication. IEEE Access 2019;7:170888–906. http://dx.doi.org/10.1109/ACCESS.2019.2955927.
[23] Li G, Boukhatem L, Zhao L, Wu J. Direct vehicle-to-vehicle charging strategy in vehicular ad-hoc networks. In: 2018 9th IFIP international conference on new technologies, mobility and security. NTMS, 2018, p. 1–5. http://dx.doi.org/10.1109/NTMS.2018.8328689.
[24] Wei Z, Li Y, Cai L. Electric vehicle charging scheme for a park-and-charge system considering battery degradation costs. IEEE Trans Intell Veh 2018;3(3):361–73. http://dx.doi.org/10.1109/TIV.2018.2843126.
[25] Masrur MA, Skowronska AG, Hancock J, Kolhoff SW, McGrew DZ, Vandiver JC, Gatherer J. Military-based vehicle-to-grid and vehicle-to-vehicle microgrid—System architecture and implementation. IEEE Trans Transp Electrification 2018;4(1):157–71. http://dx.doi.org/10.1109/TTE.2017.2779268.
[26] Kim OTT, Tran NH, Nguyen V, Kang SM, Hong CS. Cooperative between V2C and V2V charging: Less range anxiety and more charged EVs. In: 2018 international conference on information networking. ICOIN, 2018, p. 679–83. http://dx.doi.org/10.1109/ICOIN.2018.8343205.
[27] Liu S, Cao Y, Ni Q, Xu L, Zhu Y, Zhang X. Towards reservation-based E-mobility service via hybrid of V2V and G2V charging modes. Energy 2023;268:126737. http://dx.doi.org/10.1016/j.energy.2023.126737.
[28] Yuan Y, Jiao L, Zhu K, Zhang L. Scheduling online EV charging demand response via V2V auctions and local generation. IEEE Trans Intell Transp Syst 2022;23(8):11436–52. http://dx.doi.org/10.1109/TITS.2021.3103970.
[29] Koufakis A-M, Rigas ES, Bassiliades N, Ramchurn SD. Towards an optimal EV charging scheduling scheme with V2G and V2V energy transfer. In: 2016 IEEE international conference on smart grid communications. SmartGridComm, 2016, p. 302–7. http://dx.doi.org/10.1109/SmartGridComm.2016.7778778.
[30] Sehimi Y, Sakly J, Almaksour K, Robyns B. A novel fast charger architecture with reduced impact on distribution grids based on V2V power transfer. In: 2021 IEEE vehicle power and propulsion conference. VPPC, 2021, p. 1–6. http://dx.doi.org/10.1109/VPPC53923.2021.9699279.
[31] Ucer E, Buckreus R, Haque ME, Kisacikoglu M, Sozer Y, Harasis S, et al. Analysis, design, and comparison of V2V chargers for flexible grid integration. IEEE Trans Ind Appl 2021;57(4):4143–54. http://dx.doi.org/10.1109/TIA.2021.3084576.
[32] Shariff SM, Iqbal D, Alam MS, Ahmad F. A state of the art review of electric vehicle to grid (V2G) technology. IOP Conf Ser: Mater Sci Eng 2019;561(1):012103.
[33] Zhang J, Tang Q, Liu S, Cao Y, Zhao W, Liu T, Xie S. Deadline-based V2V charging under spatial resource constraints. In: 2021 international conference on control, automation and information sciences. ICCAIS, 2021, p. 240–5. http://dx.doi.org/10.1109/ICCAIS52680.2021.9624623.
[34] Liu S, Ni Q, Cao Y, Cui J, Tian D, Zhuang Y. A reservation-based vehicle-to-vehicle charging service under constraint of parking duration. IEEE Syst J 2023;17(1):176–87. http://dx.doi.org/10.1109/JSYST.2022.3145155.